Suppression of the deposition of nucleated fog droplets on steam turbine stator blades by blade heating

D. J. Ryley* and H. K. Al-Azzawi†

This is a theoretical study of the diffusive deposition of nucleated fog droplets on a low-pressure steam turbine blade operating between terminal conditions 0.23 bar, 3% wetness and 0.10 bar. Nucleation is assumed to occur at the nozzle passage entrance and fog droplets in the diameter range 0.01–1.00 μm invade both boundary layers in addition to the free stream. Droplets in the boundary layers are subject to diffusion and deposition. If the blade surface temperature is raised by internal heating, the droplets are also subject concurrently to thermophoresis and phase change. The boundary layers were divided into equal cells of size 4 mm flow-wise × 5 μm height-wise and the effects of the coupled phenomena were traced, using a comprehensive computer program, for the complete fluid transit for blade temperatures of 66–85 °C. Calculations show that deposition can be inhibited by a modest degree of heating which for 1.0 μm drops is approximately 3 kW per m of blade length.

Keywords: *steam turbines, turbine blades, thermophoresis, fog*

Erosion in a wet steam turbine commences with the deposition of nucleated fog droplets on the stator blades. Grown fog droplets usually have diameters in the range 0.01–1.0 μm and are largely immune from inertial deposition; the dominant mechanism, therefore, is diffusion. This has been studied in detail for about ten years in the Wet Steam Laboratory at the University of Liverpool using a simulation method employing aerosol particles in air. The need to use solid particles in air arose from the impossibility of distinguishing the deposition distribution of liquid particles around a steam-swept blade, all deposition history being obliterated by coalescence of the deposited water.

The initial papers[1,2] described preliminary work using a cascade of full-sized blades (the blade profile is reproduced in Appendix I) at zero incidence angle. Subsequent work explored the effects of blades at −15° incidence simulating a turbine on 75% load[3]. It was recognised at this stage that internal heating of the blade would create thermal gradients at the outside surface which might discourage diffusive deposition and this was found[4] to be the case. It was realised, however, that this work[4] could not provide satisfactory simulation of the 'real' steam case since aerosol particles, unlike fog droplets, were not subject to phase change.

To complete the series a theoretical examination has been made of the behaviour of the fog within the boundary layer, treating concurrently the principal coupled phenomena of drop phase change, diffusive deposition and thermophoresis.

* Department of Mechanical Engineering, University of Liverpool, P.O. Box 147, Liverpool L69 3BX, UK
† Mechanical Engineering Department, M.T.C., P.O. Box 478, Baghdad, Iraq. Research Student in the Department of Mechanical Engineering, University of Liverpool
Received on 3rd February 1983 and accepted for publication on 13 July 1983

Flow through the blade passage

To obtain the flow field through the blade passage we employed the familiar method of field plotting with electrically-conducting paper cut to give full size profiles. The passage centreline was taken as the locus of centres of successive circles drawn tangentially to each boundary. The flow was assumed one-dimensional along the centre-line and a sequence of flow areas found for defined values of pressure drop. At any location on the nozzle wall the flow-wise direction in the tangent plane was identified with the co-ordinate axis x and the normal to the plane with the co-ordinate axis y.

Terminal conditions for the nozzle

The first nucleation within the flow passages may occur at any location which may be found approximately by the method proposed by Gyarmathy[5]. It may be followed by a second and possibly a third nucleation. There is no 'standard position' within a stage where nucleation must occur and we therefore chose for our study a feasible set of assumptions to avoid further complicating an already complex problem. We assumed that:

1. The first nucleation occurred just upstream of the blade entry so that the entering fluid was an equilibrium mixture of saturated vapour and grown droplets, the pressure being 0.23 bar and the wetness fraction 3%, appropriate to the settled condition following the condensation shock.

 0142–727X/83/040207–11$03.00

2. The entrained droplets were monodisperse in size with a diameter in the range 0.01–1.0 μm.
3. No second nucleation occurred during the flow through the nozzle. We recognized, however, that condensation would continue to occur on the existing dispersed droplets within the core flow giving partial relief to the rising supersaturation. The method employed for calculation is described elsewhere[6] and Fig 3 shows the distribution of the temperature and wetness fraction along the core of the passage for various values of droplet size.

Boundary layer characteristics

The blade surface was assumed to be smooth and adiabatic for these calculations. Using the analysis described elsewhere[7], it was established that the lattice ratio R was large, ie the droplet population density was relatively sparse and unlikely to modify significantly the boundary layer hydrodynamic properties. Also droplets in the fog size range 0.01–1.0 μm diameter are too small to develop significant slip. It was permissible, therefore, to disregard the presence of the droplets and to calculate the boundary layer characteristics using standard methods applicable to dry flow; in our case, as explained below, the Head entrainment method[8] for turbulent boundary layers. Thwaites' method[9] was used for the laminar layer with pressure gradient and Pohlhausen's method for zero pressure gradient. The transition from laminar to turbulent flow was determined using the method devised by Abu-Ghannam and Shaw[10], for an assumed turbulence level of 2%.

Recently it has been shown that at high values of acceleration a turbulent layer undergoes a reversion to laminar flow. The derivatives $d\,Re_\theta/dx$ and $d\theta/dx$ may attain a negative value, indicating a reduction in Re_θ or θ with increasing x and a thinning in the velocity boundary layer[11]. Thus, from experiments on heated pipes, Back *et al*[12] have observed that in certain cases the reduction in heat transfer may be some 50% below the value typical of a turbulent layer. Most

Notation

A	Avogadro number
C_E	Entrainment coefficient
C_f	Skin-friction coefficient
C_p	Specific heat at constant pressure
c	Condensation coefficient, droplet population density
D	Diffusion coefficient, average spacing of adjacent droplets
d	Droplet diameter ($=2r$)
F	Cunningham correction
f	Reciprocal of droplet mobility
F_d	Damping factor
F_1	Heat transfer factor
G	Mass flux
H	Shape factor
H_1	Shape parameter
h	Enthalpy
K	Thermal conductivity
K_b	Boltzmann constant
Kn	Knudsen number
L	Acceleration parameter
$\bar{l}$	Mean free path of vapour molecules
l	Mixing length
M	Mach number
m	Mass of droplet, mass of liquid
N	Number of droplets
n	Constant in Eqs (A3)–(A6) (Appendix 2)
P	Pressure
Pr	Prandtl number
q	Heat transfer rate
R	Characteristic gas constant, rhombohedral lattice ratio
R_u	Universal gas constant
Re_x	Reynolds number based on x
Re_Δ	Reynolds number based on enthalpy thickness
Re_θ	Reynolds number based on momentum thickness
St	Stanton number
T	Absolute temperature
t	Time, temperature
U	Free stream velocity
u	Fluid velocity in x-direction
V	Droplet velocity normal to the blade surface
v	Specific volume
x	Dryness fraction, co-ordinate parallel to the blade surface
y	Wetness fraction, co-ordinate perpendicular to the blade surface
y^+	Non-dimensional y
γ	Isentropic index
Δ	Enthalpy thickness, small element
ε	Eddy diffusivity
θ	Momentum thickness
μ	Dynamic viscosity
ν	Kinematic viscosity
ρ	Fluid density

Subscripts

1	Inlet
2	Exit
av	Average
c	Transferred between cells
co	Corrected, condensation
crit	Critical
d	Diffusion
ev	Evaporation
G	Gas, vapour
L	Liquid
N	Net
o	Stagnation
p	Droplet
s	Saturation
T	Thermophoretic
u	Universal
x	Local
w	Wall, water
∞	Free stream

investigators report that the reverse transition starts at $L = L_{crit} = 3.0$ to 4.0×10^{-6} and continues while $L > L_{crit}$, L being the acceleration parameter $\nu/U_\infty^2 \times dU_\infty/dx$.

In this work, with highly accelerated flow in which $350 < (dU_\infty/dx) \lesssim 8000$, laminarization may be occurring. Calculations showed this to be the case for both concave and convex surfaces and it will be seen from Fig 1 that for both surfaces there is more than one transition, which makes interpretation more difficult. After considering the reports of a number of investigators, we adopted Head's entrainment method and solved the two main equations by computer numerical integration using the Runge–Kutta method, ie;

$$\frac{d\theta}{dx} = \frac{C_f}{2} - (H+2)\frac{\theta}{U_\infty}\frac{dU_\infty}{dx} \quad (1)$$

$$\theta\frac{dH_1}{dx} = C_E - H_1\left[\frac{C_f}{2} - (H+1)\frac{\theta}{U_\infty}\frac{dU_\infty}{dx}\right] \quad (2)$$

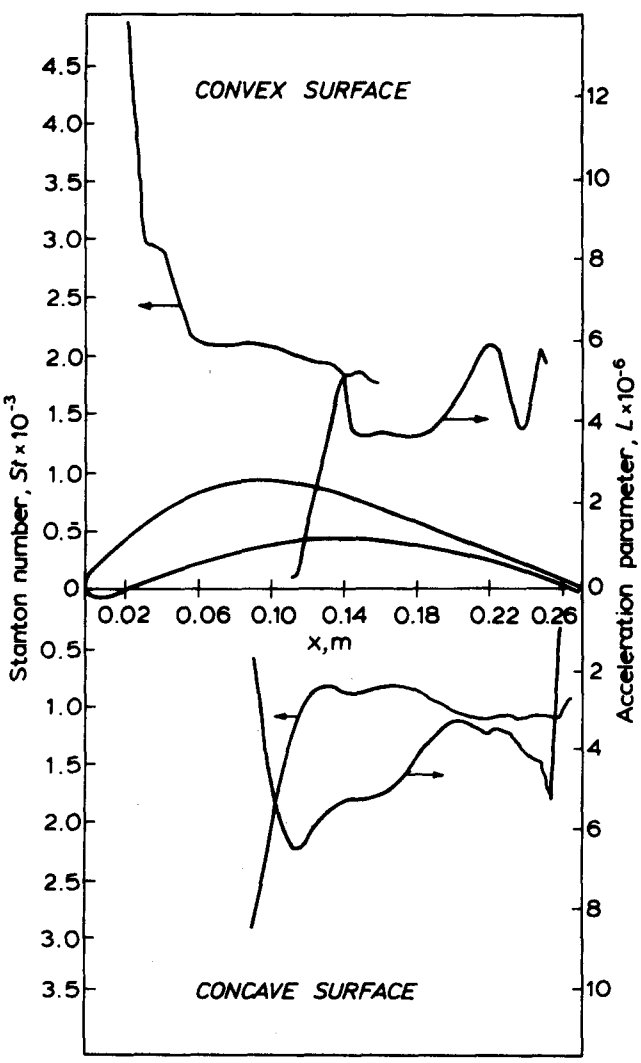

Fig 1 Blade profile, acceleration parameter and Stanton number

Heat transfer into the boundary layer

The object of this study is to determine whether phase change, leading to droplet size change, and/or thermophoretic forces, arising from thermal gradients promoted by stator blades with internal heating, will prevent the diffusive deposition of fog droplets on their surfaces. Blade heating has been studied by other workers who have seen the problem differently from ourselves. Thus Kirillov *et al*[13] investigated the combined effect of suction slots and blade heating. Deposited water was withdrawn largely by suction, any remaining being evaporated by heating. Konorski[14] addressed the problem of heating the blade surface sufficiently to evaporate all collected liquid. Engelke[15] sought to ensure heating sufficient to evaporate any deposited drops before they had time to coalesce and form rivulets. Akhtar *et al*[16] demonstrated that a single blade in a steam tunnel could be kept clear of surface water by a small amount of heating. Our view is to test the combined capacity of thermophoretic forces and evaporation of entrained droplets to ensure a dry blade surface.

For a dry flow and unit recovery factor the local temperature at the boundary will be the stagnation value. To transmit additional heat into the boundary layer it is necessary to maintain the wall temperature in excess of this value. The method due to Ambrok and modified by Moretti and Kays[17] may be used to calculate the heat transfer through a turbulent boundary layer with a variable free stream temperature and velocity. The method requires the solution of the integral energy equation which may be written for two-dimensional flow as:

$$\frac{q_w}{C_p} = \frac{d}{dx}\{\Delta G_\infty (t_w - t_\infty)\} \quad (3)$$

where

$$\left.\begin{aligned} \Delta &= \frac{\int_0^\infty \rho u (t - t_\infty)\, dy}{\rho_\infty U_\infty (t_w - t_\infty)} \\ \text{and} \quad G_\infty &= \rho_\infty U_\infty \end{aligned}\right\} \quad (4)$$

The solution is given in detail in Appendix 2 and leads to:

$$St_x = 0.0295 \frac{(t_w - t_\infty)^{0.25}\mu^{0.2}}{\left\{\int_0^x (t_w - t_\infty)^{1.25} G\, dx\right\}^{0.2}} \quad (5)$$

which can be solved numerically.

The high acceleration may reduce the intensity of turbulence and thus the rate of heat transfer. Therefore the value of St_x can be modified to $(St_x)_{co} = F_1 St_x$ where $(St_x)_{co}$ is the corrected value of St_x and:

$$F_1 = 1 - 165\left(\frac{L}{St_x}\right) \quad (6)$$

F_1 must be calculated approximately 200 θ upstream of the application point.

Fog droplets in the boundary layer

Any fog droplet in the boundary layer is subject to the following effects, all acting concurrently:

1. Flow-wise drift by vapour propulsion.
2. Mutual collision, possibly followed by coalescence, bouncing or mutual fracture.
3. Phase change. For a heated blade, this arises from thermal inertia of the droplets which are unable to adjust their temperature to rapid expansion as can the surrounding vapour. Thus the droplet temperature is usually lower than that of the vapour and evaporation occurs at the interface. There is also a small locality where condensation is found. Phase change theory is treated in Appendix 3.
4. Brownian motion. The fog droplets are sufficiently small to be moved individually by impacting vapour molecules and are thus maintained in a state of continuous random motion. This Brownian motion is intense in very small droplets, diminishes as the droplet diameter increases and eventually ceases. It is characterised by the Knudsen number, $Kn = \bar{l}/d$, becoming negligible when $Kn \sim 0.01$.
5. Diffusive deposition is due to the droplet concentration gradient multiplied by the combined effect of eddy diffusion and molecular diffusion. Eddies within the vapour transport droplets towards the boundary releasing the droplet as they die out in the sublayer.
6. Thermophoretic forces. If a droplet is within a vapour subject to a temperature gradient, the force due to molecular momentum change on the hot side exceeds that on the cooler side and the net force acts to propel the droplet 'down' the temperature gradient. A droplet, therefore, recedes from a heated surface.
7. Body forces; gravitational and centrifugal.

Fortunately, it is possible to simplify this complex problem in two ways which are both fully acceptable:

- All grown fog droplets fall within the diameter range 0.01–1.0 μm. They have negligible macroscopic slip with respect to the entraining vapour and all flow may be assumed to be homogeneous.
- The mean distance between the drops can be evaluated by assuming that each drop occupies one lattice point in a three-dimensional rhombohedral lattice. In such an event the lattice ratio R can be shown[7] to be:

$$R = \frac{D}{d} = 9\left\{\frac{x}{(1-x)\rho_G}\right\}^{1/3} \tag{7}$$

where D is the distance between drops and d the droplet diameter.

For the nozzle entry, $p = 0.23$ bar, $x = 0.97$ giving $R = 56.5$. Thus the relative spacing is very wide. The apparent mean free path $\bar{l}_p$ for a droplet of $d = 1.0$ μm is $\sim 3 \times 10^{-8}$ m and hence $\bar{l}_p/d = 0.03$, ie the mean length of droplet flight is only 3% of its diameter. For $d = 0.01$ μm, the corresponding value for this more mobile droplet is ~47%. Thus fog droplets are not only relatively far apart, their thermal mobility is also small except only for a very brief duration when the progress of evaporation has reduced their diameter to nearly zero. The issue of drop collision does not therefore arise. Deposition due to gravitational forces depends on the blade orientation and, in any case, the forces are small. Centrifugal forces are rather larger, but still small and we have neglected them. The problem therefore reduces to the simultaneous solution of effects 3, 4, 5 and 6 above.

Phase change of droplets

For a single droplet of radius r, the rate of change of r in the flow-wise direction is:

$$\frac{dr}{dx} = \frac{5.0\, Kn\, P_s}{u(1+2.7\, Kn)}\left[\frac{1}{T_G^{1/2}} - \frac{1}{T_s^{1/2}}\right] \tag{8}$$

where P_s is the local pressure of the saturated vapour, u the local velocity and T_G, T_s are respectively the vapour temperature and the vapour saturation temperature appropriate to P_s. Phase change is treated in greater detail in Appendix 3.

Diffusion and thermophoresis

Items (5) and (6) in the analysis of fog droplet behaviour indicate that diffusion propels droplets towards the heated nozzle wall but thermophoresis repels them. It is convenient, therefore, to treat analytically the combined effect. If V_N is the net deposition velocity on the wall, the basic deposition equation is:

$$cV_N = (\varepsilon + D)\frac{dc}{dy} + cV_T \tag{9}$$

where c is the droplet population concentration and V_T is the deposition velocity due to thermophoresis alone and is negative. This equation can be rewritten as:

$$V_N = \frac{V_T}{1 - \exp\left(-V_T \int_0^\infty \frac{dy}{\varepsilon + D}\right)} \tag{10}$$

and can be solved numerically. Greater detail may be found in Appendix 4.

Numerical method

The blade curvature is assumed negligible relative to the thickness of the boundary layer. In general the local conditions relevant to deposition, phase change and droplet concentration will vary both in the flow-wise (x) and the normal (y) directions. It is assumed that the droplet population is size-monodisperse at entry but during transit through the nozzle both droplets and their associated vapour undergo many variations in dynamic and thermal properties.

For this analysis the boundary layer was divided into rectangular cells stationary in space and parallel to the flow plane: cell size was 4 mm flow-wise (x-direction), 5 μm normal to the flow (y-direction)

and unity in the direction of blade length (Fig 2). The droplets within a given cell were at all times monodisperse in size and were subject to the same changes. Owing to the vast numerical population, it is impracticable to represent each droplet by a cell even if the droplet is large; hence each cell was always occupied by a set of identical droplets. It may be shown that in each cell for which the local specific volume of the mixture is v the population is:

$$N = \frac{1.432 \times 10^{-13}}{r_1^3 v} + N_c \qquad (11)$$

where N_c is the number of droplets transferred into the cell due to diffusion and thermophoresis. The accuracy of the numerical method increases as the cell size diminishes. Starting from the known conditions of droplet size and entry steam the droplet population, phase change (normally evaporation), and net motion from diffusion and thermophoresis are calculated for each cell sequentially out to the edge of the boundary layer. At each position i the difference in axial concentration between adjacent cells is calculated for the step time $\Delta t(j, i) = \Delta u_{sv}/\Delta x$. The droplet concentration at each upstream cell face in the column $j+1$ is obtained.

For the set of droplets within each cell (i, j) the following quantities are calculated: droplet size; droplet temperature; droplet velocity; droplet concentration; rate of phase change; rate of heat transfer; droplet position as a result of the coupled effects of diffusion and thermophoresis; the mass-median diameter of the population comprising the original and immigrant droplets within a cell (this defines the diameter for an equivalent monodisperse population); and droplet concentration in cell $(j+1, i)$.

This history of the changing group was traced until either all the droplets were evaporated or the residual population was discharged with the boundary layer leaving the nozzle.

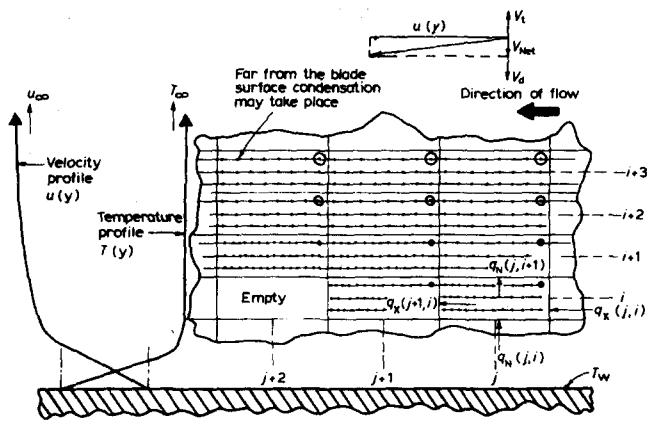

Fig 2 Notation for boundary layer cells, temperature and velocity profiles

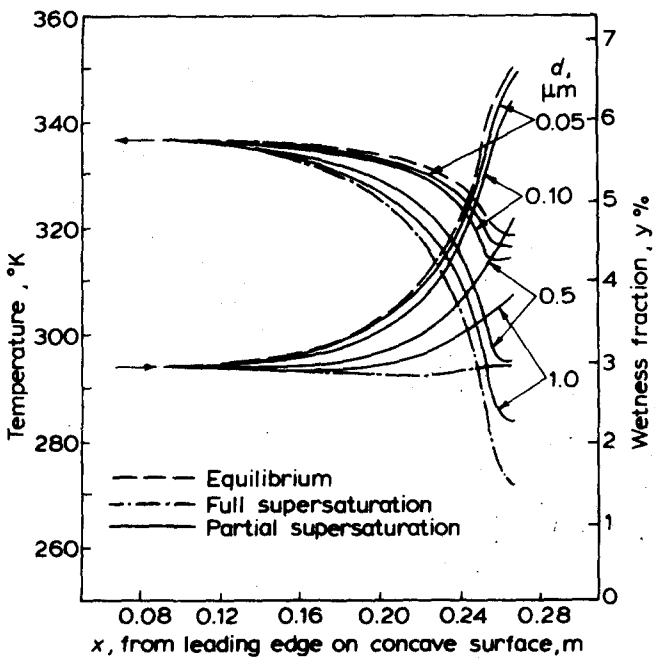

Fig 3 Core temperature and wetness fraction for a range of droplet sizes

Range of calculations

Calculations were made both for the pressure and for the suction sides of the blade using the following ranges for parametric variables: droplet size, d: 0.01, 0.05, 0.10, 0.50, and 1.00 μm; droplet path heights above the blade surface, y: 50, 100, 120, 125, 130, 300 and 450 μm; blade surface temperature, t_w: 66, 70, 75, 80 and 85 °C. The stagnation surface temperature for zero heating is 65.2 °C.

Comments and conclusions

A large number of curves[18] were computer plotted and recorded; a selection is presented here.

The lengthwise heat transfer rate into a cell adjacent to the blade surface is shown in Fig 4. The general increase occurs because, in addition to the heat received directly from the surface, heat is imported to each cell from the adjacent upstream cell, the cumulative effect increasing until the situation is disturbed near the exit by the rapid reduction in the velocity gradient dU_∞/dx which falls from ~8000 to ~3000 following the nozzle throat. The heat transfer

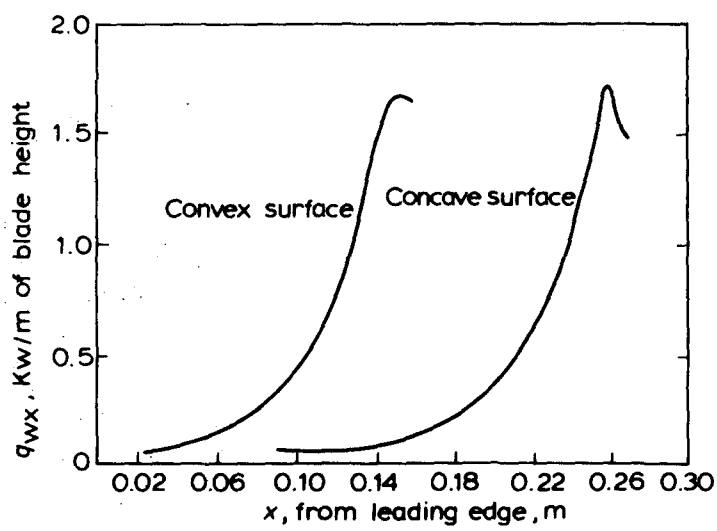

Fig 4 Heat transfer rate

rate is influenced by the nature of the boundary layer; it becomes more vigorous during turbulent flow and less so during laminar flow. It reflects, therefore, the variation in the acceleration parameter, L. The heat rate is also influenced by the local size of the fog droplet inasmuch as this size influences the local core flow temperature by relieving the supersaturation.

The mean free path, $\bar{l}$, is shown in Fig 5 for both surfaces and for both the vapour molecule and the droplet. As a droplet seldom collides with another droplet, the mean free path in this case must be interpreted as the 'apparent' mean free path[19]. Owing to evaporation (or condensation) the apparent mean free path for a droplet, as distinct from a vapour molecule,

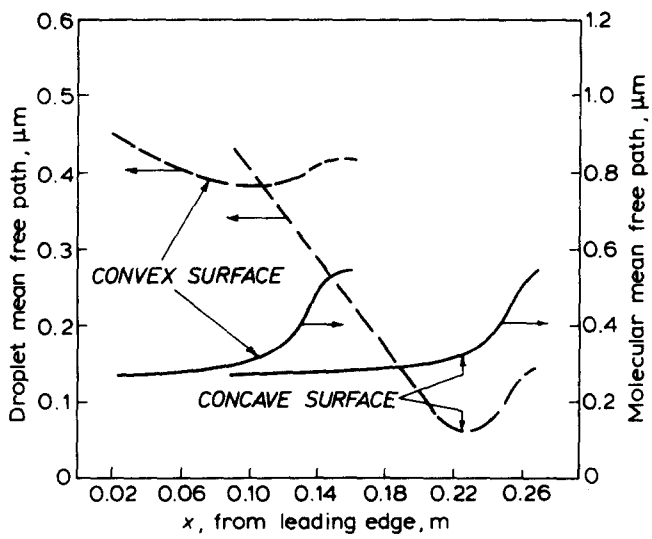

Fig 5 Molecular mean free path and droplet mean free path

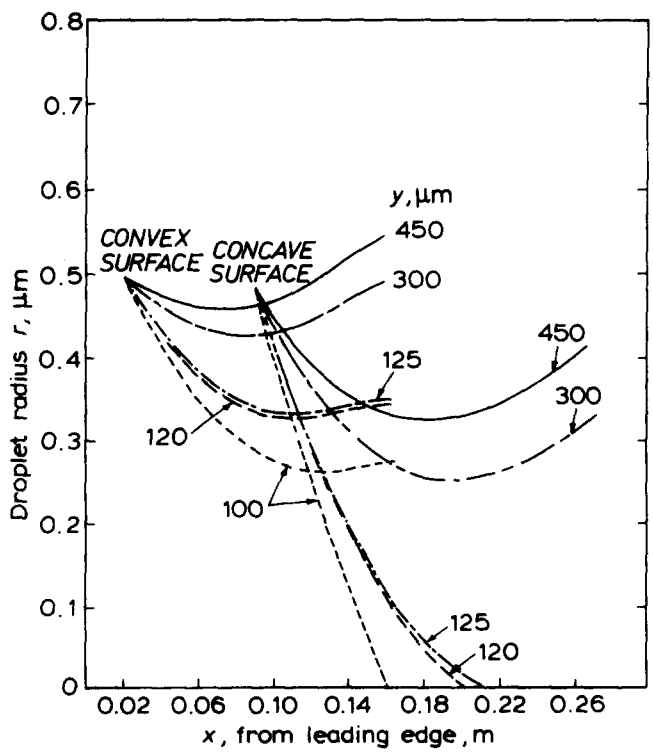

Fig 6 Droplet size history. Parameters are values of y

will vary according to its size for a given condition of the surrounding vapour. The molecular mean free path will rise with a decrease in the pressure, P_s, and the vapour density ρ_s. The same sequence of values of $\bar{l}$ for both droplet and molecule applies for the convex surface but these are displaced x-wise as a consequence of the method of measuring the locations on the two surfaces.

Fig 6 displays, for various values of y, the variation in radius of a set of droplets of initial diameter 1.0 μm during the x-transit of the concave and of the convex boundary layers. Droplets inside the cells adjacent to the heated blade surfaces are seen to evaporate completely. More remote droplets on both surfaces evaporate in varying degrees but some droplets which are far from the surface survive and grow as the nozzle exit is approached, a consequence of the diminishing core flow temperature. The corresponding local values of wetness fraction are shown in Fig 7 and the cumulative mass change in Fig 8 within an element of height $\Delta y = 5.0$ μm. Condensation is seen to occur only for droplets which are remote from the surface (large y) and hence in the cooler outer region of the boundary layer.

The values of thermophoretic velocity V_T for three selected values of y are shown in Fig 9. It is seen that droplets travelling near the wall acquire a higher thermophoretic velocity. For each surface the three curves are similar in form but V_T varies in magnitude with y. On the convex surface the curves rise slowly up to 0.12 m while on the concave surface they rise slowly up to 0.22 m. The rapid increase thereafter is due to an increase in droplet size by condensation coupled with a rising temperature gradient $(dT/dy)_x$.

The variation of the local net velocity V_N due to the combined effects of diffusion and thermophoresis is shown in Fig 10 for three values of y. When the value becomes zero no net force acts and the droplet moves parallel to the surface locally. The subsequent motion may be modified by droplet growth or evaporation.

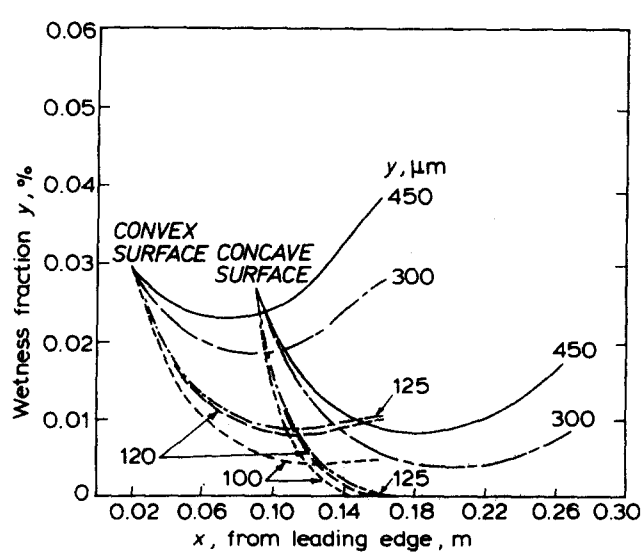

Fig 7 Wetness fraction. Parameters are values of y

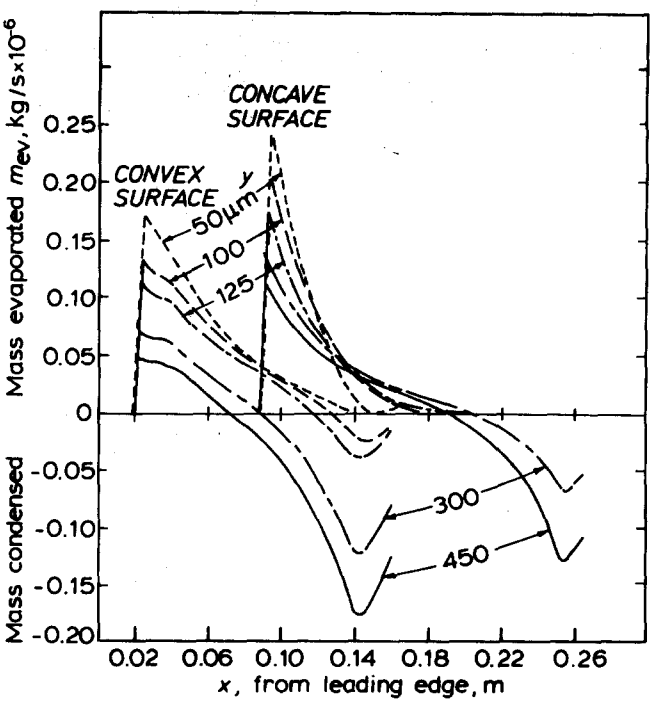

Fig 8 Mass evaporated and mass condensed (cumulative from leading edge). Parameters are values of y

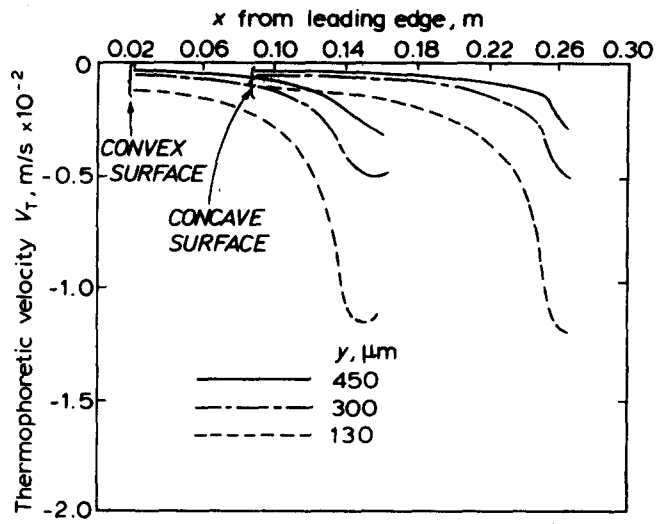

Fig 9 Thermophoretic velocity. Parameters are values of y

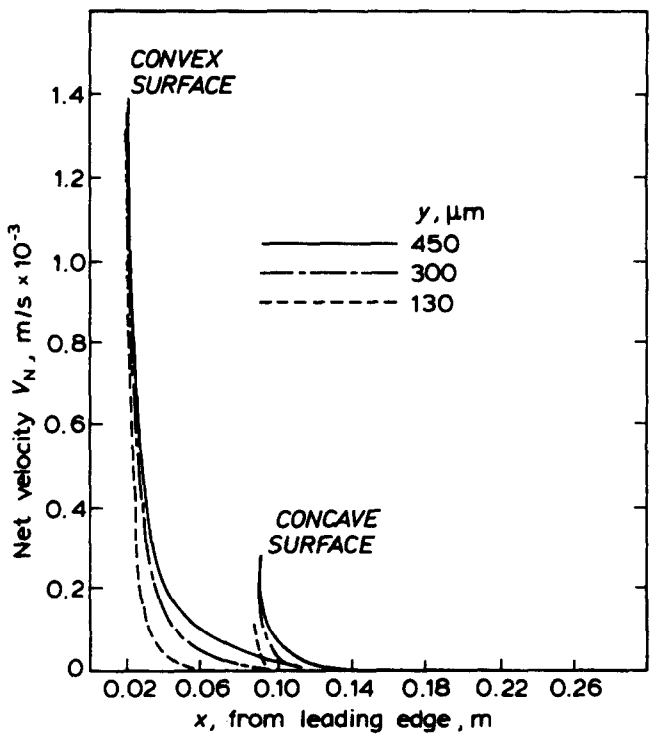

Fig 10 Net velocity (diffusion plus thermophoresis). Parameters are values of y

Fig 11 is drawn to provide a visual indication of the location of the fog 'cloud base' as the nozzle passage is traversed. Fog droplets existing 'above' the cloud base are shown conventionally as dots. The clear space immediately above the surface implies the absence of droplets and therefore of diffusive deposition and the shape and extent of this space profile depends upon the initial size of the droplet and the rate of heat input. It also differs for given conditions whether the surface considered is convex or concave. Clearly the theoretical minimum heat input is that required to lift the cloud base marginally from the entire blade surface from entry to the passage onwards to its exit.

The reader should bear in mind that all the curves shown are for the surface temperature t_w = 80 °C and for a droplet size d = 1.0 μm, where no other size is specified. This size is toward the upper end of the fog droplet size range. Smaller droplets evaporate much more quickly and the thermal load is correspondingly less for the same initial dryness fraction at passage entry.

We believe that the method and results presented here are reliable. The physical phenomena to which we have appealed, mean free path, thermophoresis, diffusive deposition and phase change of entrained droplets have all been the subject of extensive studies over many years. As stated earlier, we chose for analysis a situation in which first nucleation occurred at the nozzle entrance and not again thereafter within the nozzle. The analytical method developed is applicable in principle to the flow beyond the first nucleation wherever this occurs. It is unlikely, however, that an attempt would be made to heat rotor blading and, in any case, moving blades tend to be self-draining by centrifuging. Notwithstanding the suppression of coarse water generation which would occur after a heated fixed blade ring, it is unlikely that the beneficial effect of heating would extend much beyond the adjacent moving ring. It is now known[20], for existing turbines, that downstream of first nucleation, wherever it occurs, a confused flow situation soon supervenes and coarse water is formed.

As the main purpose of this work is to study the feasibility of stator blade heating, some conclusions bearing on this may be observed:

- For a given value of y the x-transit time is longer and the thermophoretic force is higher on the concave surface than on the convex surface. Thus droplets in the concave boundary layer have more time available for evaporation.

- The heat used in droplet evaporation is greatest at the entry section of the passage.
- Any stator blade heating would be done by steam tapped from upstream in the turbine. It would be wet saturated at the pressure appropriate to the surface temperature required, correction having been made for stagnation temperature rise. All or part of the latent enthalpy would be transferred. The mass ratio: heating steam/working steam is 0.16% for $t_w = 80\,°C$, $d = 1.0\,\mu m$. It varies with droplet size, other things being equal.
- The rate of heat input is remarkably small. Thus for a 1 m long blade of the section shown in Fig 12, the input for the whole surface is ~3 kW.

Acknowledgements

We acknowledge gratefully help given by our colleagues, Professor J. F. Norbury, Drs H. Barrow, J. L. Sproston and J. C. Gibbings and the Advisory Staff of the Computer Laboratory at Liverpool University. One of us (H. K. Al-Azzawi) is indebted to the Government of Iraq for funding as a research student during his period at Liverpool University where this work was done in the Wet Steam Laboratory, during the years 1981–1983.

References

1. **Parker G. J. and Ryley D. J.** Equipment and techniques for studying the deposition of submicron particles on turbine blades. *Proc. Instn. Mech. Engrs., 1969–70,* **184,** *(3c), 45*
2. **Parker G. J. and Lee P.** Studies of deposition of submicron particles on turbine blades. *Proc. Instn. Mech. Engrs., 1972,* **186,** *519*
3. **El-Shobokshy M. S.** Diffusional deposition of fog droplets onto L. P. steam turbine guide blades at off-design conditions. *Ph.D. Thesis, 1975, University of Liverpool*
4. **Davies J. B.** The effect of thermophoresis on the deposition of fog droplets on L.P. turbine fxed blades. *Ph.D Thesis, 1980, University of Liverpool*
5. **Gyarmathy G.** Basis for the theory of the wet steam turbine. *Dissertation E.T.H. Zurich, Juris-Verlag, 1962. English translation. C.E.G.B. (London), Rept. T.781, 1963*
6. **Ryley D. J.** Phase equilibrium in low-pressure steam turbines. *Int. J. Mech. Sci., Pergamon Press Ltd., 1961,* **3,** *28–46*
7. **Ryley D. J.** The behaviour of nucleation fogs within the nozzle boundary layer in the wet steam turbine. *J. Mech. Eng. Sci., 1971,* **13***(3), 190–199*
8. **Green J. E.** Application of Head's entrainment method to the prediction of turbulent boundary layers and wakes in compressible flow. *R.A.E. Technical Report 72079, 1972*
9. **Schlichting H.** Boundary layer theory, *7th Edn., McGraw-Hill, New York, 1979*
10. **Abu-Ghannam B. J. and Shaw R.** Natural transition of boundary layers—The effects of turbulence, pressure gradient, and flow history. *J. Mech. Engng. Sci., 1980,* **22***(5), 213–228*
11. **Back L. H., Cuffel R. F. and Massier P. F.** Laminarization of a turbulent boundary layer in nozzle flow. *A.I.A.A. J., April 1969,* **7***(4), 730–733*
12. **Back L. H., Massier P. F. and Cuffel R. F.** Some observation on reduction of turbulent boundary layer heat transfer in nozzles. *A.I.A.A. J., 1966,* **4***(12), 2226–2229*
13. **Kirillov I. I., Nosovitskii A. I. and Shpenzer G. G.,** Moisture removal by separation and evaporation in wet turbine stages. *Teploenegetika. (Translated from Russian), 1970,* **17***(8), 40–42*
14. **Konorski A.** Steam drying in condensing turbines by internal preheating method utilising its own steam. *Gdansk. Prace Instytutu Maszyn Prezeplywowych, 1962, pp. 63–119*

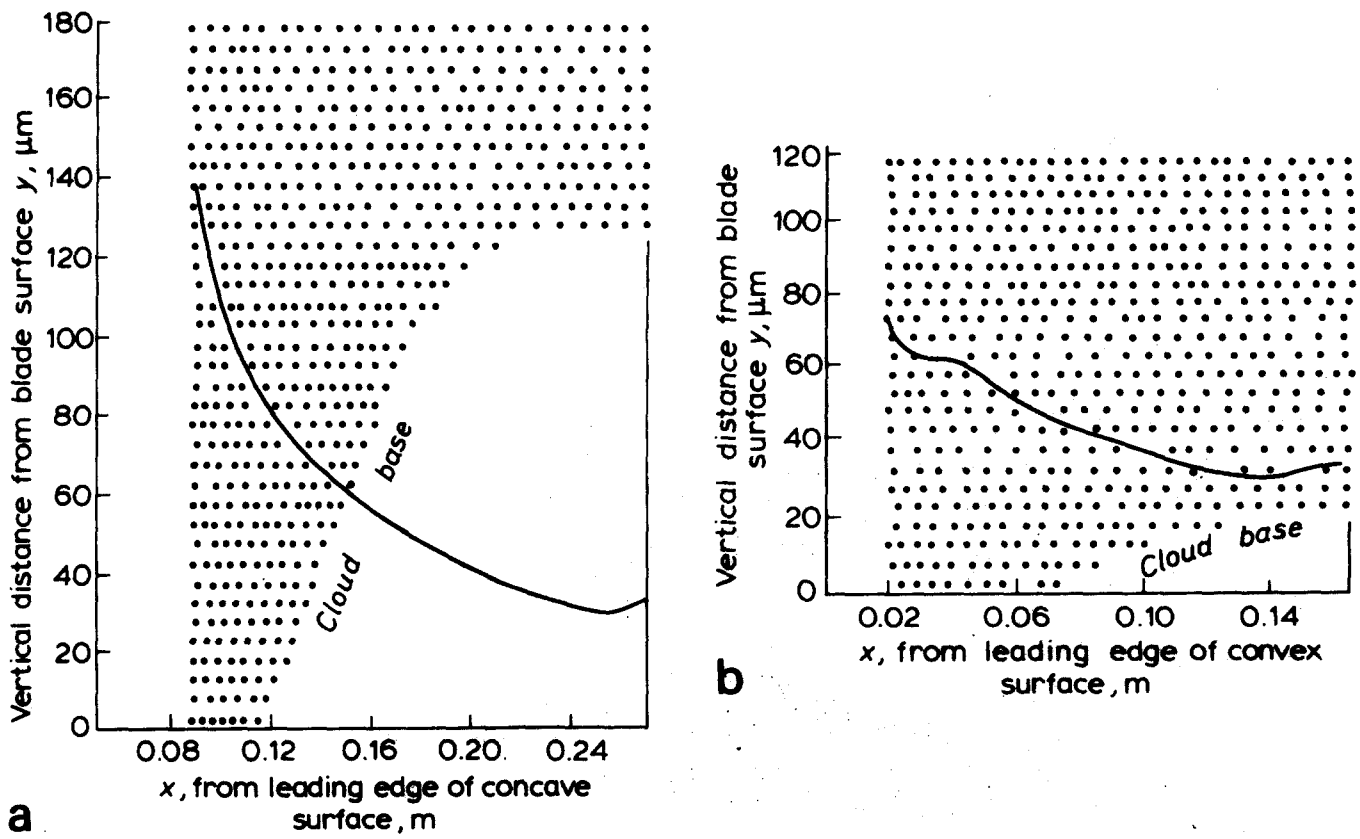

Fig 11 Profile of fog droplet cloud base and of boundary sublayer (a) Concave surface (b) Convex surface

15. **Engelke W.**, Operating experience of wet steam turbines. *in Two-phase steam flow in turbines and separators. (Eds. Moore M. J. and Sieverding C. H.), McGraw-Hill Book Company, 1976, pp. 305–311*
16. **Akhtar M. S., Black J. and Swainston M. J. C.** Prevention of steam turbine blade erosion using stator blade heating. *Proc. Instn. Mech. Engrs., 1977,* **191***(17/77), 355–361*
17. **Moretti P. M. and Kays W. M.**, Heat transfer to a turbulent boundary layer with varying free-stream velocity and varying surface temperature; an experimental study. *Int. J. Heat & Mass Transfer, 1965,* **8**, *1187–1202*
18. **Al-Azzawi H. K.** Postgraduate work in hand in the Wet Steam Laboratory, University of Liverpool.
19. **Fuchs N. A.** The mechanics of aerosols. *Pergamon Press, 1964*
20. **Gyarmathy G. and Spengler P.** Flow fluctuations in multistage steam turbines. *(Eds P. Suter and G. Gyarmathy) Traupel-Feschrift, Zurich, 1974*
21. **Young J. B.** Nucleation in high pressure steam and flow in turbines. *Ph.D. Thesis, University of Birmingham, 1973*
22. **Annis B. K., Malinauskas A. P. and Mason E. A.** Theory of drag on neutral or charged spherical aerosol particles. *J. Aerosol Sci., 1972,* **3***(1), 55–64*
23. **Lin C. S., Moulton R. W. and Putnam G. L.** Mass transfer between a solid wall and fluid streams. *Ind. Engr. Chem., 1953,* **49***(1), 636*
24. **Van Driest E. R.** On turbulent flow near a wall. *J. Aero. Sci., 1956,* **23**, *1007–1012*
25. **Talbot L., Cheng R. K., Schefer R. W. and Willis D. R.** Thermophoresis of particles in a heated boundary layer. *J. Fluid Mech., 1980,* **101***(4), 737–758*

Appendix 1

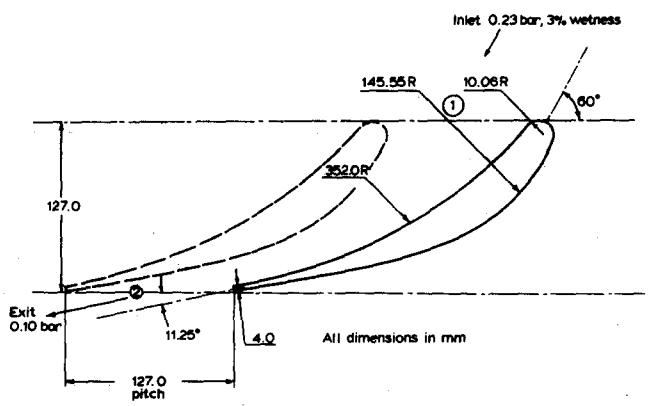

Fig 12 Blade dimensions and operating conditions

Appendix 2. Heat transfer into the boundary layer

The integral energy equation for two-dimensional flow is:

$$\frac{q_w}{C_p} = \frac{d}{dx}\{\Delta G_\infty (t_w - t_\infty)\} \tag{A1}$$

where:

$$\left.\begin{aligned} \Delta &= \frac{\int_0^\infty \rho u (t - t_\infty)\, dy}{\rho_\infty U_\infty (t_w - t_\infty)} \\ \text{and} \quad G_\infty &= \rho_\infty U_\infty \end{aligned}\right\} \tag{A2}$$

or, expressed as a function of x:

$$\Delta = \frac{c U_\infty^{-n}}{\nu^{-n}} \frac{x^{1-n}}{1-n} \tag{A3}$$

The integral energy equation can be written as:

$$\left\{\frac{1-n}{c}\right\}^{(2n-1)/(n-1)} \mu^{1/(1-n)} G (t_w - t_\infty)^{1/(1-n)}\, dx = d\{G\Delta(t_w - t_\infty)\}^{1/(1-n)} \tag{A4}$$

Also, St can be defined as a function of Δ thus:

$$St_x = c\left\{\frac{1-n}{c}\right\}^{n/(n-1)} Re_\Delta^{n/(n-1)} \tag{A5}$$

Then by substituting Δ into the integral energy equation

$$St_x = \frac{c(t_w - t_\infty)^{n/(1-n)} \mu^n}{\left\{\int_0^x (t_w - t_\infty)^{1/(1-n)} G\, dx\right\}^n} \tag{A6}$$

where $c = 0.0295\, Pr^{-0.4}$ and $Pr \approx 1.0$ and $n = 0.2$
Therefore:

$$St_x = 0.0295 \frac{(t_w - t_\infty)^{0.25} \mu^{0.2}}{\left\{\int_0^x (t_w - t_\infty)^{1.25} G\, dx\right\}^{0.2}} \tag{A7}$$

Appendix 3. Kinetic expression for change of phase in droplets

At low pressures small droplets do not significantly distort the molecular velocity distribution in the adjacent vapour and it is usual to employ an analytical method based on the kinetic theory of gases. There are several variants of this method and that employed here is due to Young[21]. From kinetic theory, the mass of vapour molecules impinging on the interface in unit time is:

$$\frac{4\pi r^2 P_G}{(2\pi T_G)^{1/2}}$$

Let c be the fraction of the impinging molecules that adheres to the interface (condensation) and $1-c$ the fraction that rebounds. The rate of condensation is:

$$\frac{dm_{co}}{dt} = \dot{m}_{co} = \frac{4\pi r^2 P_G c}{(2\pi R T_G)^{1/2}} \tag{A8}$$

Using a similar argument for the molecules approaching the interface from the liquid side, the mass/unit time which escapes through the interface (ie evaporates) is:

$$\dot{m}_{ev} = \frac{4\pi r^2 P_L c}{(2\pi R T_L)^{1/2}} \tag{A9}$$

The quantity c is called the condensation coefficient and is taken to have the same value for both condensation and evaporation. Combining Eq (A8) and (A9):

$$\frac{dm}{dt} = \dot{m}_{co} - \dot{m}_{ev} = \frac{4\pi r^2 c}{(2\pi R)^{1/2}}\left[\frac{P_G}{T_G^{1/2}} - \frac{P_L}{T_L^{1/2}}\right]$$

which gives:

$$\frac{dm}{dt} = cr^2\left(\frac{8\pi}{R}\right)^{1/2}\left[\frac{P_G}{T_G^{1/2}} - \frac{P_L}{T_L^{1/2}}\right] \quad \text{(A10)}$$

since $m = 4\rho_w/3\pi r^3$ this may be written:

$$\frac{dr}{dx} = \frac{2}{3}\frac{1}{\pi u \rho_w} \cdot \frac{Kn}{\left(1+\frac{2.7\,Kn}{c}\right)}\left(\frac{8\pi}{R}\right)^{1/2}\left[\frac{P_G}{T_G^{1/2}} - \frac{P_L}{T_L^{1/2}}\right] \quad \text{(A11)}$$

To solve equation (A11) c is taken as 1.0, R for steam as 461.5 J/kg K; $P_G \simeq P_L \sim P_S$, the saturation pressure; $T_L = T_S$, the saturation temperature and $\rho_w = 1000$ kg/m^3. Inserting these values, Eq (A11) reduces to

$$\frac{dr}{dx} = \frac{5.0\,Kn\,P_S}{u(1+2.7\,Kn)}\left[\frac{1}{T_G^{1/2}} - \frac{1}{T_S^{1/2}}\right] \quad \text{(A12)}$$

Appendix 4. Diffusion and thermophoresis

For coupled diffusion and thermophoresis in the turbulent boundary layer the deposition equation is:

$$cV_N = (\varepsilon + D)\frac{dc}{dy} + cV_T \quad \text{(A13)}$$

For the laminar boundary layer ε is set equal to zero in equation (A13). The molecular diffusion coefficient D is given by:

$$\left.\begin{aligned} D &= \frac{K_b T}{f} \\ \text{where} \\ f &= \frac{6\pi r\mu}{F} \end{aligned}\right\} \quad \text{(A14)}$$

The Boltzmann constant $K_b = R_u/A = 1.381 \times 10^{-23}$ J/K where R_u is the universal gas constant, A is the Avogadro number $= 6.033 \times 10^{23}$, f^{-1} is the particle mobility and F is the Cunningham correction. The form of F here used is due to Annis *et al*[22]:

$$F = 1 + Kn[1.558 + 0.173\exp(-0.769/Kn)] \quad \text{(A15)}$$

The eddy diffusivity of the droplet, ε, was taken to equal that of the steam, an acceptable assumption for small droplets. In contrast to previous studies where the boundary sublayer only was treated[3,4,23] we have employed here the Van Driest[24] model to find the value of ε throughout the entire boundary layer:

$$\varepsilon = l^2\left|\frac{du}{dy}\right| \quad \text{(A16)}$$

where

$$\left.\begin{aligned} l &= 0.4y[1 - F_d] \\ \text{and} \\ F_d &= \exp^{-1}(y^+/26) \end{aligned}\right\} \quad \text{(A17)}$$

For thermophoresis an expression due to Talbot *et al*[25] may be used over the whole range of Knudsen number:

$$V_T = -\frac{2C_S\nu\left(\frac{K_G}{K_p} + C_t\frac{l}{r}\right)\left[1 + \frac{l}{r}\left[A + B\exp\left(-\frac{Cr}{l}\right)\right]\right]\left(\frac{dT}{dy}\right)_x}{\left(1 + 3C_m\frac{l}{r}\right)\left(1 + 2\frac{K_G}{K_p} + 2C_t\frac{l}{r}\right)T_{av}}$$

where $C_S = 1.14$, $C_t = 2.18$, $C_m = 1.14$, $C = 0.88$, $A = 1.2$, $B = 0.41$ and $K_G/K_p = 0.03$.

BOOK REVIEWS

Combustion in Engineering

These two volumes are a collection of 37 research papers presented at an international conference organised by the Institution of Mechanical Engineers, and attended by some 130 delegates from many different countries, at Keble College, Oxford in April 1983. The volumes are A4 size, 'paper-back' form, and although the type-face differs from paper to paper the format is consistent and the general appearance is uniform.

Taken together, the volumes are intended to provide 'a comprehensive up-to-date review of combustion in engineering'. There is certainly a wide variety of topics covered (perhaps too wide for any one person to have a specific interest in more than a small proportion of the papers) as would be expected from so wide a subject. It is debatable, however, whether a cohesive and complete 'state-of-the-art' picture can be built up in this manner.

Each of the volumes is also considered to be 'complete in itself' though it is unlikely that a potential buyer would want half of a complete story and the topics covered in the two volumes do inevitably overlap to some extent. Individuals, one would expect, would also be less likely to buy a collection of widely ranging papers (at £25) than, say, the library or reference section of a university or an automotive or power industry concern.

Volume 1 consists of twenty papers (200 pages) taken from the first half of the conference in which the topics covered included instrumentation and diagnostic techniques, ignition mechanisms, mathematical modelling and turbulence in combustion in both engines and rigs. Volume II contains the remaining papers (164 pages) of the second half of the conference and topics included are internal combustion engines and gas turbines, fuels, and combustion in furnaces.

The papers are, in general, clearly presented with diagrams and graphs appearing at the end of each paper and with standard units used (almost) throughout. Since the papers were prepared for the conference delegates, the discussions which took place after each session are unfortunately absent.

R J Crookes
Queen Mary College, London, UK

Published, price £15 per volume or £25 for the set in the UK (£19.50 and £32.50 respectively elsewhere) by Mechanical Engineering Publications Ltd., PO Box 24, Northgate Avenue, Bury St Edmunds, Suffolk IP32 6BW, UK